Vol. 2, No. 1, pp. 7-11, June 2003

INTERNATIONAL JOURNAL OF SAFETY
www.kiis.or.kr

A Numerical Study on Methane-Air Counterflow Diffusion Flames Part 1. Concentration of Fuel

Woe Chul Park*

Department of Safety Engineering, Pukyong National University, Busan 608-739, Korea

(Received March 27, 2003; Accepted May 30, 2003)

Abstract : Structure of the counterflow nonpremixed flames were investigated by using Fire Dynamics Simulator (FDS) and OPPDIF to evaluate FDS for simulations of the diffusion flame. FDS, employed a mixture fraction formulation, were applied to the diluted axisymmetric methane-air nonpremixed counterflow flames. Fuel concentration in the mixture of methane and nitrogen was considered as a numerical parameter in the range from 20% to 100% increasing by 10% by volume at the global strain rates of $a_g = 20\ s^{-1}$ and $80\ s^{-1}$ respectively. In all the computations, the gravity was set to zero since OPPDIF is not able to compute the buoyancy effects. It was shown by the axisymmetric simulation of the flames with FDS that increasing fuel concentration increases the flame thickness and decreases the flame radius. The centerline temperature and axial velocity, and the peek flame temperature showed good agreement between the both methods.

Key words : counterflow flame, methane, zero gravity, fuel concentration, flame thickness, flame radius

Nomenclature

a_g : global strain rate
L : separation distance between ducts, 15 mm
R : radius of duct, 7.5 mm
t : thickness of duct wall, 0.5 mm
V_A : air velocity at duct exit
V_F : fuel velocity at duct exit
ρ_A : density of air
ρ_F : density of fuel

1. Introduction

The structure and extinction of hydrocarbon diffusion flames are important in development of agents for fire suppression. Among experimental studies on the counterflow flames, Maruta *et al.* [1] and Park *et al.* [2] recently studied low and moderately strained flames in microgravity condition. The exprimrents were carried out through drop tests to investigate the methane-air diffusion flames with nitrogen gas added to the fuel stream where buoyancy forces are negligible. On the other hand, numerical studies on such low strain rate flames have been performed by using the one-dimensional flame codes OPPDIF [3], which was developed based on a similarity solution that neglects buoyancy.

A numerical method is needed that is able to simulate buoyancy dominated flows and is easily extended to multi-dimensional dynamics to investigate physical insights of the counterflow flames. The NIST Fire Dynamics Simulator (FDS) [4], developed mainly for computing unsteady three-dimensional large-scale fire phenomena by employing a large eddy simulation (LES) turbulence model, in which the resolvable large-scale eddies are computed directly and the sub-grid dissipative processes are modeled. FDS also employs the direct numerical simulations (DNS) for small-scale problems like the counterflow flames. The latter is more suitable for the diffusion flames than the large eddy simulations, computing directly transport and dissipative process. Though FDS with DNS have been utilized to the counterflow flames [2, 5-8], more investigations are in need in a wide range of fuel concentrations and global strain rates. The objective of this study is to investigate agreement between FDS and OPPDIF for different fuel concentrations in the nitrogen-diluted fuel stream with comparisons of the computed results of the two methods. The diffusion flames were simulated in zero gravity conditions since OPPDIF is not capable of pre-

*Corresponding author: wcpark@pknu.ac.kr

dicting the buoyancy effects. The effects of fuel concentration on the flame thickness and radius were also investigated by using FDS.

2. Methodology

The counterflow burner has two opposed circular ducts separated by a distance L as shown in Fig. 1. A mixture of fuel and agent (nitrogen) is supplied through the lower fuel duct, and air flows in the oxidizer duct. R is the radius of duct, t is the thickness of duct wall. Dimensions of L, R, and t are 15 mm, 7.5 mm, and 0.5 mm, respectively.

Combustion is assumed to take place in quiescent nitrogen gas. The oxidizer is composed of pure air and the fuel is composed of a mixture of methane and nitrogen. The numerical parameter, methane concentration in the fuel duct, varies from 10% to 100% increasing by 10% by volume for the global strain rates of 20 s^{-1} and 80 s^{-1}, respectively.

The top hat velocity profile was imposed at the both duct exits, no slip condition on the duct walls, and T = 25°C in fuel and air streams. The velocity boundary conditions were investigated in detail by Park and Hamins [6]. The solution procedures are described in detail in McGrattan *et al.* [4] and Park and Hamines [8].

Based on an evaluation procedure, the computational domain was taken to be 40 mm in both the r and y directions. The grid spacing was taken to be 0.5 mm in the r and y directions, corresponding to 80×80 grids. Since a steady state flame was obtained in about 0.7 s, computations were carried out up to 1.0 s, and the average temperature and axial velocity along the center line (y axis) were calculated from the instantaneous values of 0.8~1.0 s.

For a given global strain rate, a_g, the velocity of the oxidizer stream (air) V_A and that of fuel stream (mixture of methane and nitrogen) V_F at the duct exits are calculated by the definition of the global strain rate,

$$a_g = \frac{2V_A}{L}\left[1 + \frac{V_F}{V_A}\left(\frac{\rho_F}{\rho_A}\right)^{0.5}\right] \quad (1)$$

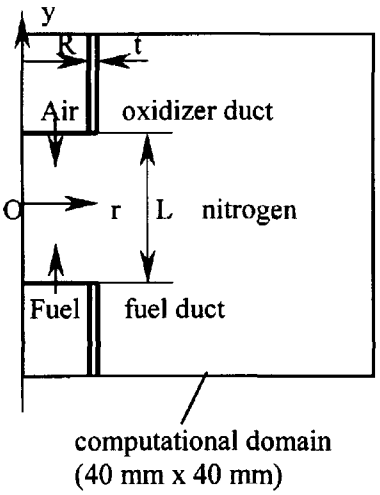

Fig. 1. Schematic of the counterflow burner.

3. Results and Discussion

3-1. Low Strain Rate (a_g= 20 s^{-1})

Fig. 2 compares the flames simulated by FDS at a_g = 20 s^{-1} for the methane concentrations of 20% (N_2 80%) and 80% (N_2 20%) in the fuel stream. The flame of methane 20% is much thinner than that of methane 80% while the diameter of the fuel lean flame is larger than that of the fuel rich flame. The flame thickness and radius measured from the isotherm of 1000°C were 2.8 mm and 19.4 mm for methane concentration of 20%, and 4.8 mm and 16.6 mm for methane

concentration of 80%, respectively. These results show that increasing fuel concentration increases the flame thickness and decreases the flame radius. The differences in flame thickness and radius appear to be caused by reaction between methane and oxygen. Note that compar-

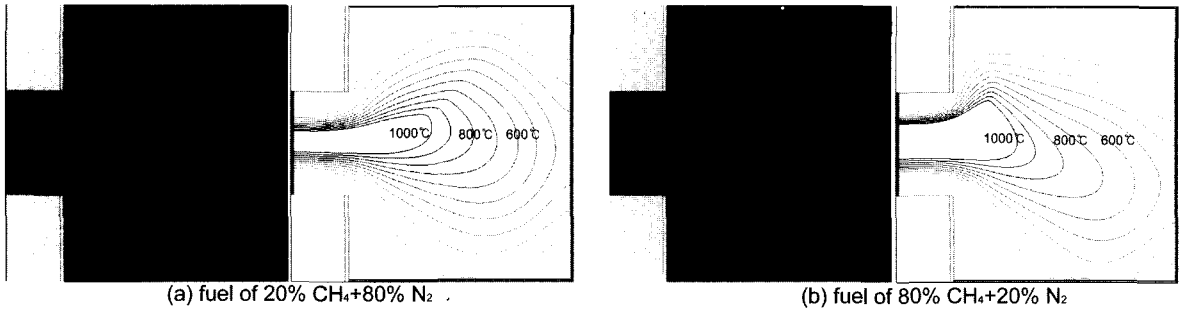

Fig. 2. Flames at a_g= 20 s^{-1} (FDS)

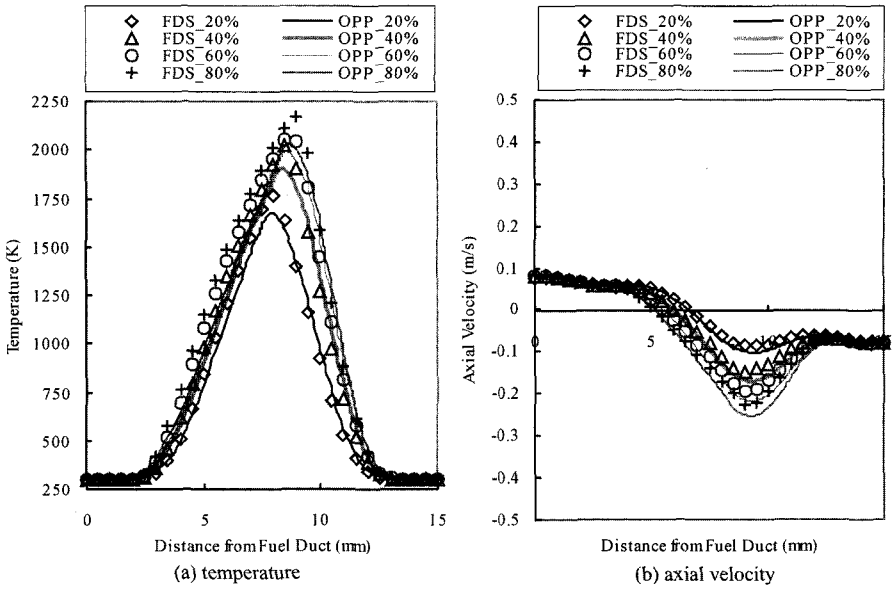

Fig. 3. Comparison of temperature and axial velocity for fuel concentrations at $a_g = 20\ s^{-1}$.

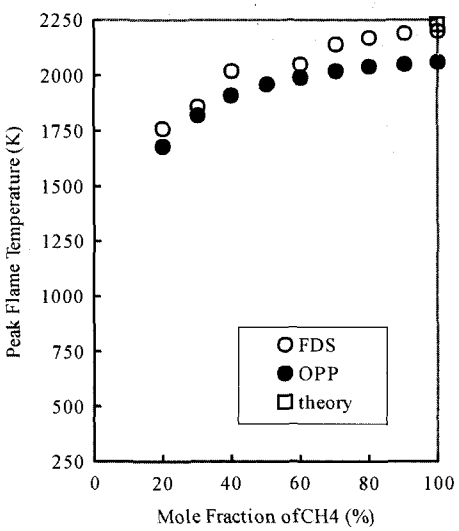

Fig. 4. Comparison of peak flame temperature for fuel concentrations at $a_g = 20\ s^{-1}$.

isons between FDS and OPPDIF are not possible since OPPDIF can not provide the flame shape.

The corresponding temperature and axial velocity along the duct centerline were compared in Fig. 3 for methane concentrations of 20, 40, 60, 80% in the fuel stream. Although difference in the peak flame temperature increases with the fuel concentration, the temperature profiles of the two methods are in good agreement. It also show that the flame temperature increases with the fuel concentration. The axial velocity distributions along the centerline are also in good agreement for all the fuel concentrations.

Fig. 4 compares the peak flame temperature for the fuel concentration between FDS and OPPIDIF at the low strain rate. FDS predicts the peak flame temperature better than OPPDIF though the temperature of the fuel concentration 40%. is too high. For the undiluted methane (CH_4 100% in fuel stream), FDS yielded 2200 K which is very close to the theoretical value, 2227 K [9] while OPPDIF did 2062 K.

3-2. Moderate Strain Rate ($a_g = 80\ s^{-1}$)

The flames of $a_g = 80\ s^{-1}$ for the methane concentrations

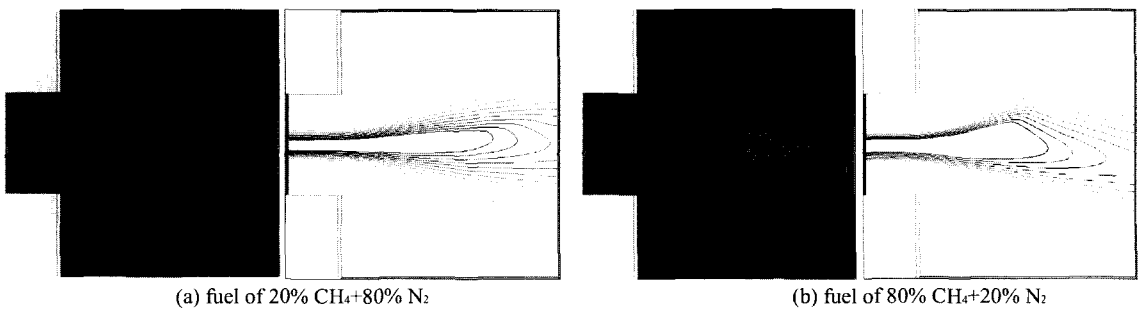

Fig. 5. Flames at $a_g = 80\ s^{-1}$ (FDS).

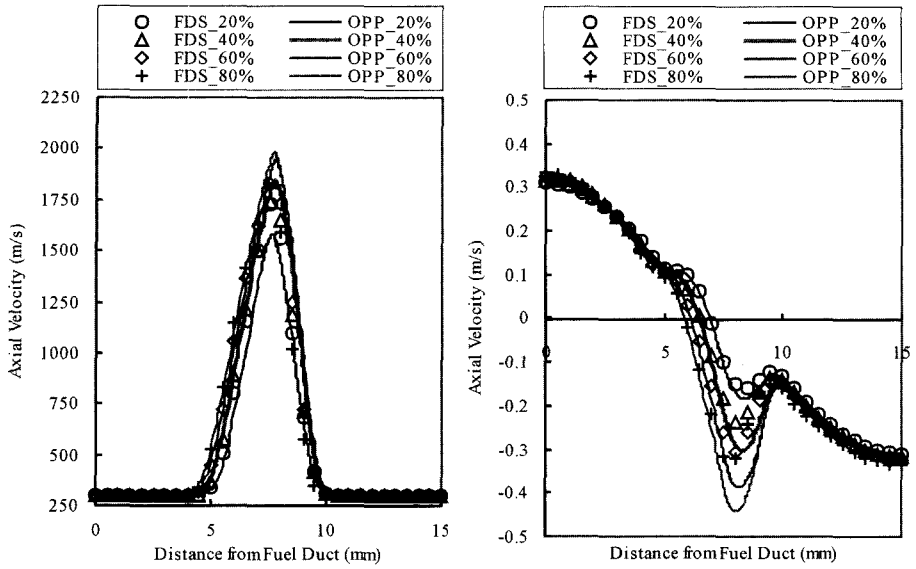

Fig. 6. Temperature and axial velocity for fuel concentrations at $a_g = 80\ s^{-1}$.

of 20% and 80% were compared in Fig. 5. The change in the flame thickness and radius at $a_g = 20\ s^{-1}$ is also observed in this moderate strain rate, that is, the flame thickness and radius measured from the isotherm of 1000°C were 1.3 mm and 29.5 mm for the methane concentration 20%, and 1.8 mm and 26.3 mm for the methane concentration 80%, respectively. The flame thickness increases with the fuel concentration, and the flame radius decreases as the fuel concentration increases. Compared to the low global strain rate case shown in Fig. 2, the flame is much thinner and its diameter is larger at the higher global strain rate.

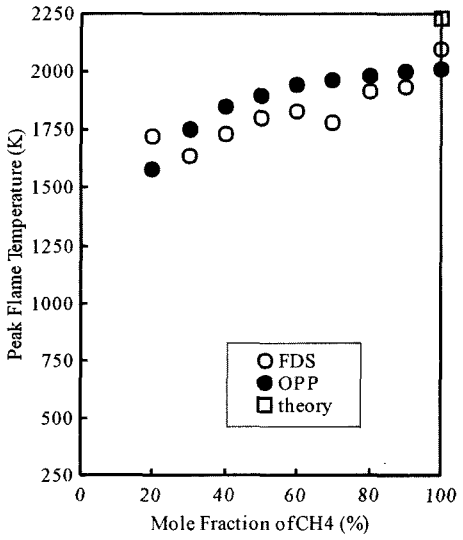

Fig. 7. Comparison of peak flame temperature for fuel concentrations at $a_g = 80\ s^{-1}$.

Fig. 6 compares the temperature and axial velocity profiles along the duct centerline for methane concentrations of 20, 40, 60, 80% in the fuel stream at $a_g = 80\ s^{-1}$. For low methane concentrations both FDS and OPPDIF are in good agreement in the temperature and axial velocity. Despite difference between FDS and OPPDIF increases with the fuel concentration, FDS well predicts the effects of the fuel concentration on the temperature and axial velocity profiles.

Fig. 7 shows the peak flame temperature for different values of the fuel concentrations. The peak temperature increases with the fuel concentration to the theoretical temperature [9]. Though the peak temperatures of FDS at the methane concentrations of 20% and 70% are scattered, FDS predicts the peak temperature better than OPPDIF for the 100% methane without the nitrogen agent in the fuel stream.

4. Conclusions

The nitrogen diluted counterflow methane-air diffusion flames were simulated using FDS and OPPDIF for the fuel concentrations in the range from 20% to 100% to evaluate FDS. It was shown by FDS that the flame thickness increases and flame radius decreases with increasing fuel concentration. The temperature and axial velocity profiles along the duct centerline of FDS agreed well with those of OPPDIF. FDS predicted more accurate peak flame temperature for all the fuel concentrations computed at $a_g = 20\ s^{-1}$ and for 100% methane in the fuel stream at both $a_g = 20\ s^{-1}$ and $80\ s^{-1}$ compared with OPPDIF.

Acknowledgement

This work was supported by Pukyong National University Research Fund in 2002.

References

[1] K. Maruta,, M. Yoshida, H. Guo, Y. Ju and T. Niioka, "Extinction of Low-Streched Diffusion Flame in Microgravity", Combustion and Flames, Vol. 112, pp. 181~187, 1998.

[2] W. C. Park, A. Hamins, M. Bundy, K. Y. Lee and J. Logue, "Structure and Suppression of Low Strain Rate Nonpremixed Flames", Submitted to Trans. Korean Institute of Fire Science & Engineering, 2003.

[3] A. Lutz, R. J. Kee, J. Grcar and F. M. Rupley, "A Fortran Program Computing Opposed Flow Diffusion Flames", SAND96-8243, Sandia National Laboratories, Livermore, CA, U.S.A., 1997.

[4] K. B. McGrattan, H. R. Baum, R. G. Rehm, A. Hamins, G. P. Forney, J. E. Floyd and S. Hostikka, "Fire Dynamics Simulator Technical Reference Guide", v.3, National Institute of Standards and Technology, Gaithersburg, MD, U.S.A., 2002.

[5] W. C. Park, "An Evaluation of a Direct Numerical Simulation for Counterflow Diffusion Flames", J. of KIIS, Vol. 16, No. 4, pp. 74~81, 2001 (in Korean).

[6] W. C. Park and A. Hamins, "Investigation of Velocity Boundary Conditions in Counterflow Flames", KSME Intl J., Vol. 16, pp. 262~269, 2002.

[7] W. C. Park and K. C. Ko, "investigation of Effects of Duct Thickness on Counterflow Flame Structure", J. of KIIS, Vol. 17, No. 4, pp. 61~65, 2002 (in Korean).

[8] W. C. Park and A. Hamins, "Development of a Three-Dimensional DNS Code for Study of Clean Agents - Two-Dimensional Simulation of Diluted Nonpremixed Counterflow Flames", Intl. J. of Safety, Vol. 1, No. 1, pp. 18~23, 2002.

[9] T. Baumeister, E. A. Avallone and T. Baumeister III, Marks Standard Handbook for Mechanical Engineers, 8th ed., McGraw-Hill, p. 4~57, 1978.